Int. J. Electrochem. Sci., 11 **(2016)** 9355 – 9368, doi: 10.20964/2016.11.66

International Journal of ELECTROCHEMICAL SCIENCE
www.electrochemsci.org

The Anodic Excursion Peak as a Rapid Way of Measuring the Corrosion of Lead Alloys

J. Lach[1], *A. Czerwiński*[2,3,*]

[1] Industrial Chemistry Research Institute, Rydygiera 8, 01-793 Warsaw, Poland
[2] Faculty of Chemistry, Warsaw University, Pasteura 1, 02-093 Warsaw, Poland
[3] Biological and Chemical Research Centre, University of Warsaw, Zwirki i Wigury 101, 02-089 Warsaw, Poland
[*]E-mail: aczerw@chem.uw.edu.pl

Received: 9 August 2016 / *Accepted:* 17 September 2016 / *Published:* 10 October 2016

The corrosion of the positive plate is an important aspect of the lead-acid batteries behavior. Having a fast and reliable way of testing it would improve the process of upgrading and designing new lead-acid batteries. For this reason the relationship between the corrosion resistance of lead alloys and their anodic excursion peaks was investigated. First tests were conducted on disc electrodes made of lead alloys, for which the excursion peaks were measured. Different samples made of the same alloys were corroded electrochemically. Results show that there is a correlation between the excursion peak current and the weight loss during the anodic corrosion of lead-antimony and lead-tin alloys. Moreover, this correlation was confirmed for a complete 2 V lead-acid battery with collectors made from a commercially used multi-component alloy. The excursion peak is also very similar for solid lead electrodes and electrodes from lead electroplated on reticulated vitreous carbon, which shows that the proposed measurement can be used for lead-acid batteries with reticulated current collectors. The main advantages of the described way of investigating the lead alloy corrosion are: fast measurement and small amount of material required.

Keywords: lead acid batteries, corrosion, lead alloys, anodic excursion peak, reticulated vitreous carbon

1. INTRODUCTION

The lead acid battery is one of the oldest and still very widely used battery type in the modern world. Currently, they are often used as backup power supplies and also in the automotive industry, both as SLI (Starting, Lighting, Ignition) and traction batteries. One of the reasons that allows their diverse applications is the possibility of modifying their electrochemical properties by using different lead alloys in their current collectors (grids). Pure lead has been replaced with lead alloys to improve

the mechanical properties of the material, like hardness and castability. The alloys can also improve the grid corrosion resistance by using the appropriate additives. The grid corrosion is a very important problem as it is one of the main reasons of a battery failure. One of the first widely used additives was antimony. It increases the alloy hardness, but also decreases the hydrogen overvoltage. The latter property increases the water loss during the battery operation, which is then needed to be periodically refilled. With the spread of VRLA and low maintenance batteries low-antimony alloys gained popularity. The low-antimony alloys required addition of elements like sulfur or selenium, which act as grain refiners. In other cases the antimony was completely phased out of alloy, like in the lead-tin alloys. The addition of other elements like silver, cobalt, cadmium or calcium can also improve the alloy behavior. The currently used alloys have multiple additives, which helps them achieve desired properties [1-3].

When one develops a new type of a lead-acid battery, he must choose the alloy composition most suited to the proposed application. However, there is a multitude of available additive combinations. Additionally, there is still room for improvement in the currently used alloys, by adding new alloying elements or by optimizing the amounts of additives used. One of the problems in introducing a new alloy is the necessity of measuring the corrosion resistance of the considered composition in a fast and reliable way. Multiple methods are employed to this end, with a weight loss of an alloy being a commonly measured parameter. The disadvantage of these tests is that they typically take a lot of time, requiring usually a few days [4-7]. Having a fast method for measuring the corrosion of lead alloys simplifies the process of selecting a new alloy or improving an existing one.

This work studies the rate of weight loss during the corrosion of lead alloys and its correlation with the anodic excursion peak of lead. The excursion peak is a known phenomena in the lead electrochemistry. It is an anodic peak, appearing during the reduction of a lead electrode. The electrode needs to be previously oxidized to generate a corrosion layer, consisting mostly of PbO_2. The excursion peak lays very close to the reduction peak of PbO_2. Since its discovery there were multiple attempts at explaining the mechanism causing the peak appearance [8-15].

The theory presented first by Deutcher et al. in 1986 assumes that the excursion peak is a result of oxidation of the metallic lead under the corrosion layer. This lead is exposed during the PbO_2 reduction because of the changes in molar volume during the transition from PbO_2 to $PbSO_4$. This reaction puts a considerable pressure on the corrosion layer, which causes its cracking. These cracks can be deep enough to reach the unoxidized lead of the electrode [11].

If the excursion peak is indeed dependent on the structure of the corrosion layer, like its thickness or compactness, then there will be a connection between the peak and the anodic corrosion resistance of a lead material. In the course of this study we examined the excursion peak current for different lead alloys and compared it with the rate of weight loss during anodic corrosion.

2. EXPERIMENTAL

2.1. Electrode preparation

Tin and antimony alloys for the measurements were prepared from chosen elements, which have been mixed and melted together. Lead with a purity of 99.94%, manufactured by Innovator

(Poland), was used. Tin (99.85% pure) was made by Chempur (Poland). Antimony had a purity of 99.88% and was produced by Onyxmet (Poland). Two types of binary alloys were prepared: lead-tin and lead-antimony, with the additive amount in 0.5 – 5 wt% range. Five different lead-tin alloys had the following tin content: 0.5% (PbSn 0.5%), 1.0% (PbSn 1%), 2.0% (PbSn 2%), 2.5% (PbSn 2.5%), 5.0% (PbSn 5%). The lead-antimony alloys had antimony content of: 0.5% (PbSb 0.5%), 1.0% (PbSb 1%), 1.5% (PbSb 1.5%), 2.5% (PbSb 2.5%), 5.0% (PbSb 5%). Each series of electrodes was cast in a shape of a rod, with 5 mm diameter and 50 mm long. Afterwards the rods were kept in 200˚C for two hours. The rods where then rolled to assure the proper shape. Some of the rods were covered in epoxy resin and used as a disc electrodes. The rest of the rods, after shortening to the length of 30 mm, was used in the weight loss measurements.

2.2. Weight loss measurements

The weight loss measurements were conducted in a two-electrode system. The counter electrode was a lead foil surrounding the working electrode – an lead alloy disc electrode. The electrolyte was 4.9 M H_2SO_4 (37.5 wt%). The whole system was kept in a thermostated water bath at a temperature of 50ºC. The working electrode was corroded by applying a constant anodic current of 100 mA for 24 hours. Afterwards, the sample was removed from the vessel and the corrosion layer was dissolved, using the solution of 100 g NaOH and 20 g sucrose per 1 liter of water. Finally the sample was washed and dried. The electrode was weighed before and after the experiment and the mass difference was measured. For an uncorroded lead sample the weight did not change. Similar method was already used before in other publications [16-18].

2.3. Excursion peak measurements

The excursion peak was measured in a three-electrode vessel. The counter electrode was again a lead foil and the electrolyte was 4.9 M H_2SO_4 (37.5 wt%). The reference electrode was a mercury sulfate electrode, $Hg|Hg_2SO_4|1M\ H_2SO_4$. All potentials in this paper are reported versus its potential (660mV vs. SHE). The working electrode was a disc electrode prepared from the chosen lead alloy. The measurement was conducted in three phases, as described in an earlier patent [19]. First the electrode surface needed to be prepared. The electrode was polished with an abrasive paper (grade P 1200), then it was placed in the vessel and reduced for 3 minutes at the constant potential of -1.4 V. The second phase consisted of generating the oxide layer. It was done by polarizing the electrode at the constant potential of 1.2 V for 30 minutes. In the third step, the excursion peak was measured using the linear sweep voltammetry, with the potential changing from 1.2 V to 0.7 V at a sweep rate of 5 mV/s.

2.4. Lead-acid battery tests

The positive plate grids for the lead-acid battery were cast using two lead alloys. The first one had the following additives: Sb 3%, Sn 0.3%, As 0.2%, Cu 0.01% (alloy M1). The second had similar

composition with only the Sb content increased to 6% (alloy M2). The negative plates were made of pure lead. Both types of plates had been pasted with an appropriate active material and subsequently seasoned and formed. One positive and one negative plate were connected in a 2V cell with the capacity of 2 Ah. Two batteries with two different alloys (M1 and M2) in the positive plate were constructed. The electrolyte used was 4.9 M H_2SO_4 (37,5 wt%).

The tests on lead-acid batteries were performed by a cyclic discharge and charge. The battery was discharged with the C/4 current for 1 hour and the voltage at the end of this step was recorded. Then it was charged for 2h 55m at the constant voltage of 2.47 V, followed by 5 minutes of charging at the constant current of 2.5C/20. These conditions are similar to one used by manufacturers in lead-acid battery cycle life test.

2.5. Scanning Electron Microscope (SEM)

Morphology of corrosion on a reticulated and solid electrode was examined using SEM, model JEOL JSM-6490LV. The solid electrode was made from a slice of rod similar to those used in the weight loss measurement. The reticulated electrode was prepared by electrodeposition of lead on a Reticulated Vitreous Carbon (RVC) matrix. The method of this electrodeposition was described in our earlier paper [20]. The samples were prepared using cyclic voltammetry. They were cycled 90 times back and forth between the potential of 0.45 and 1.45 V, at the 50 mV/s sweep rate. After reaching 1.45 V in the final cycle the samples were washed with distilled water, dried and placed in SEM chamber.

3. RESULTS AND DISCUSSION

3.1. Weight loss and excursion peak correlation

The weight loss during the anodic corrosion for lead-tin and lead-anitmony alloys was measured as described in section 2.2.

Table 1. The weight loss during the anodic corrosion for the lead-tin and the lead-antimony alloys with different additive concentrations.

Alloy	Pb	PbSn 0.5%	PbSn 1%	PbSn 2%	PbSn 2.5%	PbSn 5%
Weight loss [%]	1.37	1.12	1.03	0.93	0.91	0.37
Alloy	PbSb 0.5%	PbSb 1%	PbSb 1.5%	PbSb 2.5%	PbSb 5%	
Weight loss [%]	1.32	1.32	1.22	1.19	1.60	

The results in Table 1 show that for the lead-antimony electrodes the increase in the antimony concentration initially lowers the weight loss, but this loss rises again after a minimum for the Pb-Sb 2.5% alloy. For the lead-tin alloys with increasing tin content the weight loss constantly decreases.

The excursion peak for these alloys was also measured, as described in the section 2.3. The general shapes of voltammograms in the excursion peak region for these two types of alloys are shown in Fig. 1.

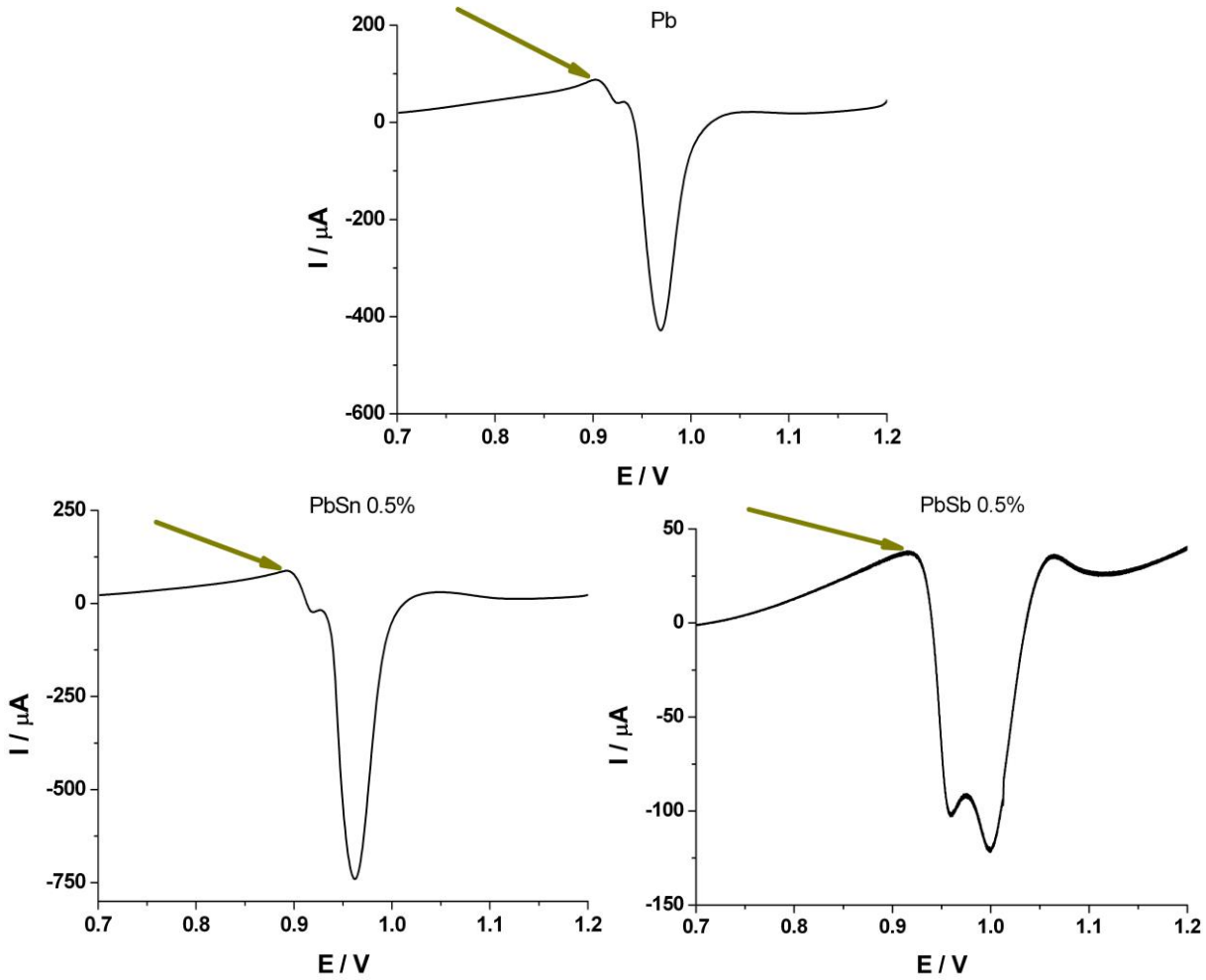

Figure 1. The excursion peak region for the lead, lead-antimony and the lead-tin alloy with the 0.5% additive concentration. Arrows point to the excursion peak.

The alloying element concentration has a great influence on the shape of the measured excursion peak. In case of the lead alloyed with antimony one can clearly see two reduction peaks, that are the result of reduction of two PbO_2 polymorphs, alpha and beta. The excursion peak overlaps with those peaks. For the lead-tin alloys the reduction peak at higher potential is much larger. Fig. 2. shows how the region of the excursion peak changes with increase in the additive concentration.

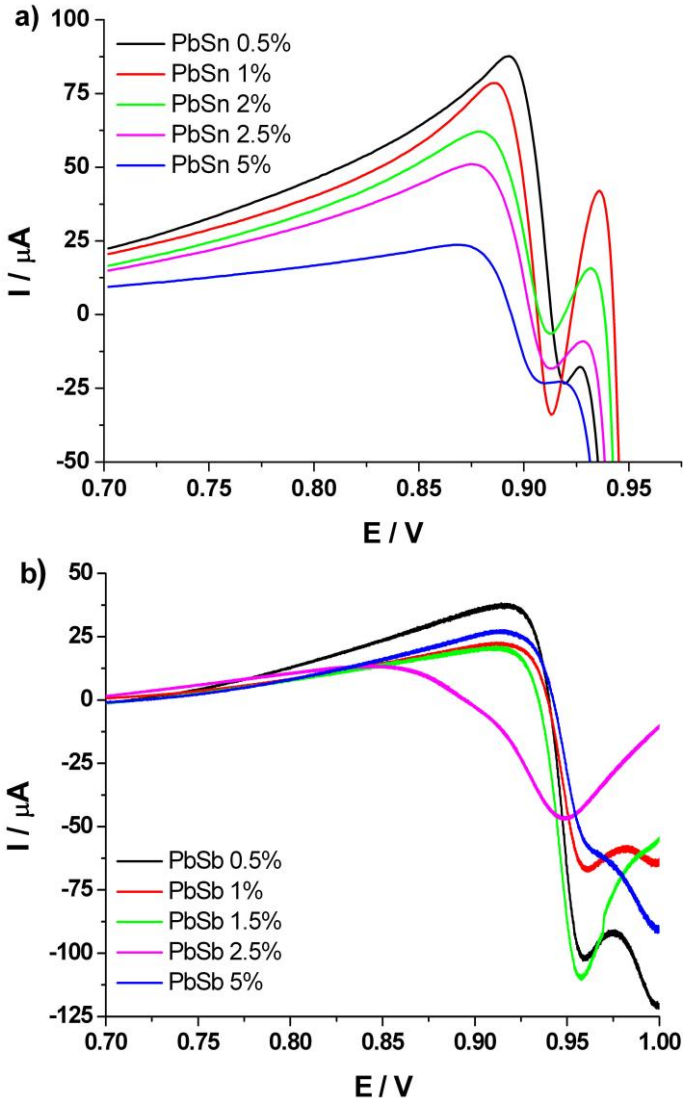

Figure 2. The excursion peak for the lead-tin (a) and lead-antimony (b) alloy with different additive concentrations.

It can be seen that the changes in the size of the excursion peak follow the same tendency as the changes in the weight loss in the examined alloys. For the alloys with increasing antimony content, the excursion peak decreases, until it reaches minimum at the 2.5% Sb content, when it starts to increase again. For the lead-tin the excursion peak is clearly decreasing with the increase in the tin content, just as the weight loss did.

The currents of the excursion peaks were taken from these measurements. These currents were then compared with the alloy weight loss during anodic corrosion. The obtained results are presented in Fig. 3.

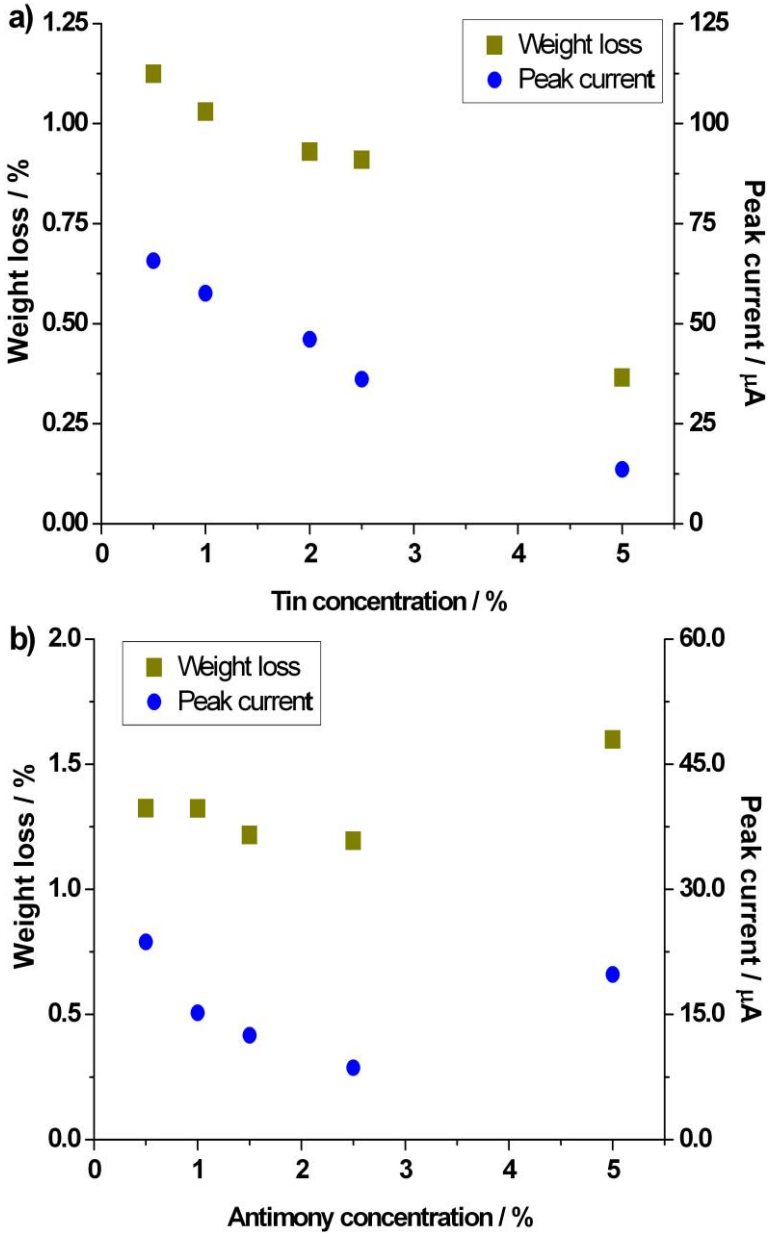

Figure 3. The comparison of the excursion peak current and weight loss during anodic corrosion for lead-tin (a) and lead-antimony (b) alloys.

The graph in Fig. 3. clearly shows that alloys with a higher tin content exhibit a lower weight loss, so they have a higher corrosion resistance. This fact is not a surprise, as lead-tin alloys are in general considered more corrosion-resistant [21]. The addition of tin changes the properties of a passive layer, and some research shows that alloys with a tin content lower than 1% have insulating PbO layer, and only further addition causes it to get thinner and more conductive [22, 23]. However, this will not necessarily will be reflected in the amount of weight loss during our experiment, as even small tin additions (below 1%) were reported to improve other properties of the alloy, like the initial charge acceptance and early-life cycling capacity [24, 25]. Measurements conducted by other researchers for lead-tin alloys with addition of calcium (even as low as 0.06% Ca) are also in

agreement with our results. The decrease in the weight loss for alloys with a higher tin content was reported even for low tin concentrations [7, 26]. Other parameters like the polarization resistance, the reduction time of the corrosion layer and the microstructure of the alloy also show improvements for a low tin content [27, 28].

The weight loss measured by us for the lead-antimony alloys is initially dropping with the increase in the antimony content and reaches a minimum for PbSb 2.5%, with the following PbSb 5% alloy having increased corrosion. The literature reports the best cycle life for lead-antimony alloys with a high antimony content (over 6%) [1, 3]. Research for low-antimony alloys shows however, that an increased antimony content even in a low range, below 5% improves the corrosion resistance [29-31]. The results obtained by us are in agreement with earlier research, with the exception of the high corrosion rate for the PbSb 5% alloy. There are, however, some other results showing lower capacity for alloys with Sb content of 4.5% than for alloys with Sb content of 1.8% [32]. For our measurement this discrepancy for PbSb 5% alloy could be explained by the method of preparation of electrodes, as they were rolled during their production. Rolled antimony alloys have worse corrosion behavior and mechanical properties than cast alloys, especially for higher antimony content [33], which would explain the high corrosion rate of the PbSb 5% alloy.

Overall, the graphs in Fig. 3. show that there is indeed a correlation between the excursion peak and the weight loss during corrosion. The changes in these two values follow each other for both lead-antimony and lead-tin alloys. This result confirms that the current value of the excursion peak can be used to compare the corrosion resistance of lead alloys with a different concentration of the alloying element.

3.2. Lead-acid battery measurements

Further measurements were conducted on 2V lead-acid cells to investigate whether the results for rods cast from alloys will translate to results for complete batteries.

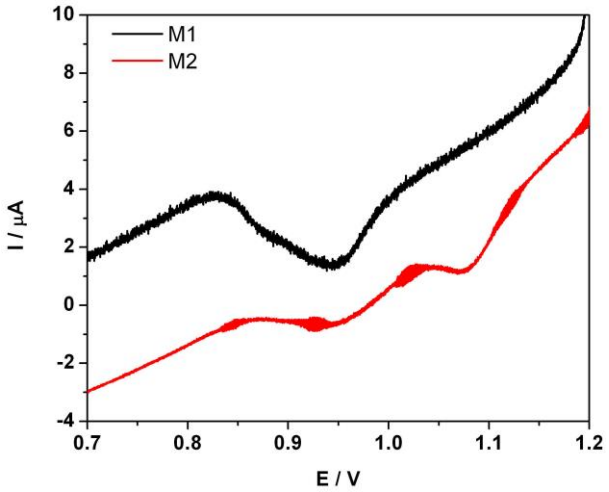

Figure 4. The excursion peak for the multi-additive alloy M1, and the alloy M2 with increased Sb content.

For these tests two alloys with multiple alloying elements were used, as described in section 2.4. Disc electrodes were also prepared from these two alloys for comparison. First the excursion peaks for these electrodes were measured in a similar way as the lead-tin and lead-antimony measurements.

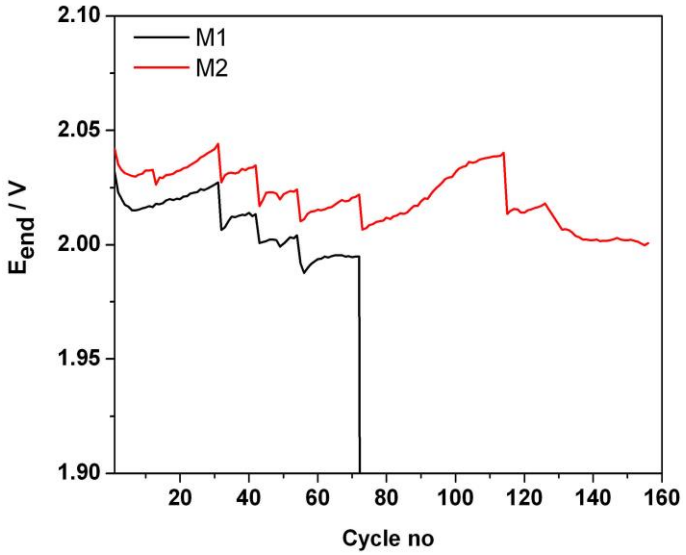

Figure 5. The voltage at the end of discharge during cycling of the 2V cells made of M1 and M2 alloys.

The plots in Fig. 4. shows that the alloy M2 has a much smaller excursion peak. Based on this result the corrosion resistance for alloy M2 is expected to be greater. To confirm this hypothesis two cells were prepared, the first one using the M1 alloy and the second using the M2 alloy. These cells were cycled in the conditions described in section 2.4, which allows us to compare the corrosion resistance of the M1 and M2 alloys. The voltages at the end of discharge during consecutive cycles are shown in the Fig. 5.

The plots in the Fig. 5. have a few sharp drops in voltage between cycles for both cells. These are caused by refilling the cells with distilled water, as the conditions of the test caused intense electrolyte loss. The cell with the M1 alloy grid had overall lower discharge voltages during completed cycles, moreover it completely failed after the 73rd cycle due to the corrosion. The cell with the M2 alloy had completed around 150 cycles with higher voltages, and was still working as the test was ended. The worse performance of the battery with the lower antimony content (with the M1 grid) is not surprising, as high antimony alloys were widely used to decrease the corrosion of flooded lead-acid batteries. Alloys having the traditionally used 6-11% antimony content have a better cycle life compared to the alloys with a lower antimony content [1, 3]. Results for the M1 and M2 alloys therefore confirm the assumption, that the excursion peak is correlated with the corrosion of a lead-acid battery.

3.3. Reticulated current collector measurements

An additional field where the investigated method can be used are the reticulated current collectors. They are collectors made of carbon, used in lead-acid batteries in place of typical grids. They are lighter and have a bigger surface area, which leads to a higher specific energy and increase in the active material utilization. The reticulated carbon collector can be electroplated by lead or lead alloy. The carbon material used can be RVC [20, 34-39], a pitch-based carbon foam [40-43], a carbon honeycomb grid [44-46] or a graphite foam [47]. Measuring the excursion peak can be a cheap and fast method of evaluating the usefulness of lead alloys as a plating on this type of collectors. The SEM image of Pb/RVC collector is shown in Fig. 6.

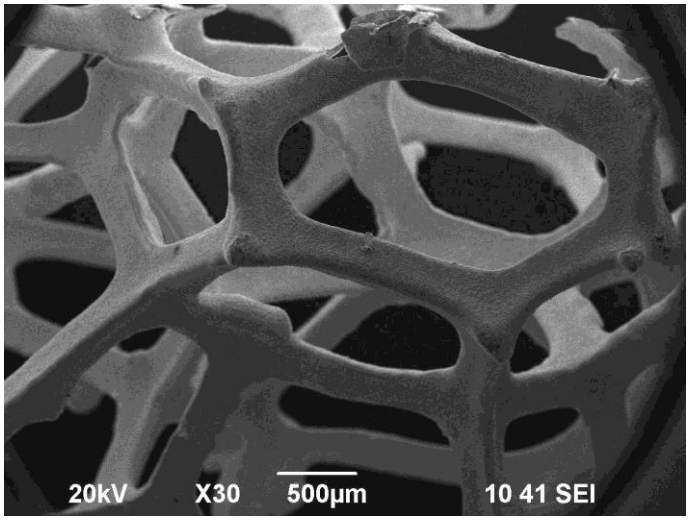

Figure 6. The SEM photograph of Pb/RVC collector electroplated with lead.

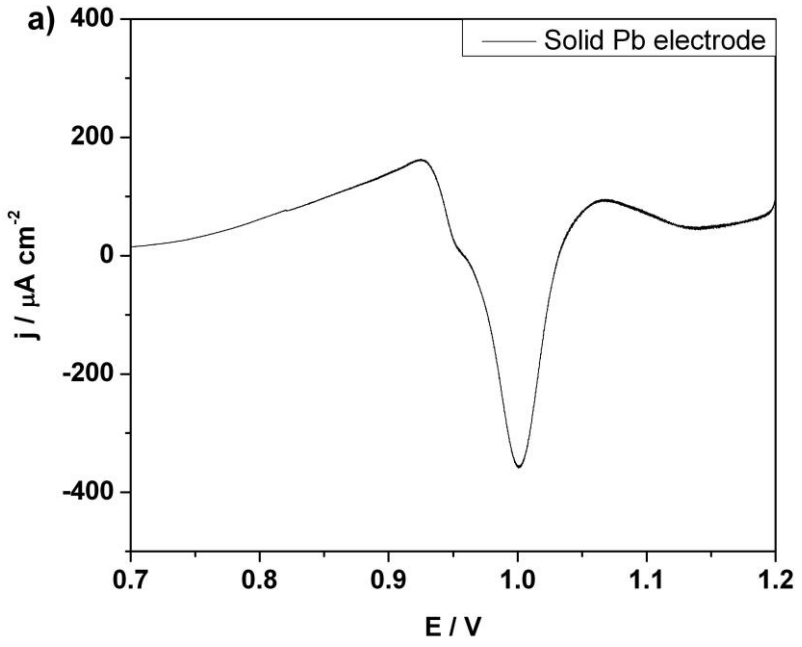

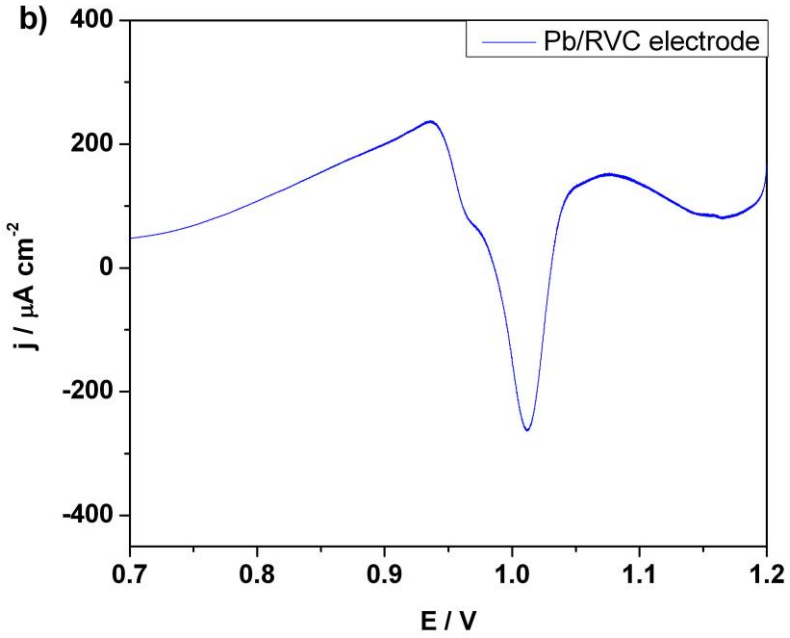

Figure 7. The excursion peak for solid (Pb) and reticulated (Pb/RVC) lead electrode.

The measurement of the excursion peak was conducted, exactly as described in section 2.3 with piece of reticulated collector used as a working electrode in place of a disc electrode. Fig. 7. shows the comparison of the excursion peak for the reticulated collector and a solid electrode made of pure lead.

One can see that for the reticulated collector the excursion peak is still present. It also retains very similar shape as the peak on the solid electrode. This result is in agreement with the previous study indicating similarities in the electrochemical properties of metallic lead and lead electrodeposited on RVC [34].

The morphology of the corrosion layer on the reticulated electrode was also examined using SEM. A thick corrosion layer, similar to one formed in batteries, was prepared using the cyclic voltammetry as described in section 2.5.

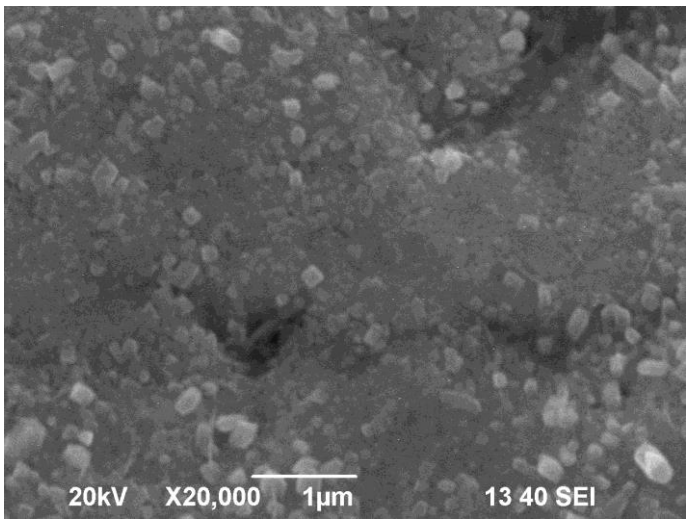

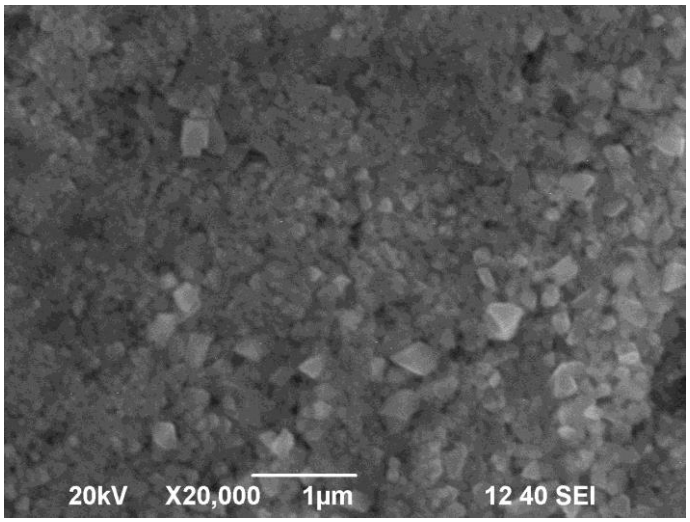

Figure 8. The corrosion layer on a solid Pb (left) and a reticulated Pb/RVC (right) electrode.

A solid and a reticulated electrode were used. Fig. 8. shows that the corrosion layer for both cases is very similar. We see a compact layer of PbO_2 with comparable grain size.

The overall results for both types of electrodes show that the behavior in the excursion peak region is very similar in both cases. This leads us to believe that the proposed method of investigating the corrosion resistance of alloys can be also successfully used for the reticulated collectors.

4. CONCLUSIONS

In this study we investigated the correlation between the excursion peak and the weight loss during the anodic corrosion of lead alloys. The excursion peak for binary lead-tin and lead-antimony alloys with different additive concentrations was investigated. The weight loss during the anodic corrosion of these alloys was also measured. The comparison of the excursion peak current and the weight loss shows a clear correlation between these them. We also studied whether the correlation between the excursion peak and the alloy corrosion is preserved in complete lead-acid batteries. To this end we investigated the corrosion of 2V lead-acid cells with grids made from two different multi-component alloys. The end results are in agreement with predictions resulting from the excursion peak observation of these alloys. Finally, the excursion peak behavior for reticulated collectors (Pb/RVC) was examined. The excursion peaks for the solid and the reticulated electrode are very similar. Also SEM images show a clear resemblance between corrosion layers on these two types of electrodes. The excursion peak measurements therefore can be used to evaluate the corrosion resistance of a lead alloy. This test can be used in the research in the lead-acid battery industry, it would be a progress in traditional methods of gravimetric measurements of the weight loss of an alloy. The advantages are: much quicker measurement (few tens of minutes compared to days) and usage of only a small amount of the examined material. It can be used both for the introduction of new alloys or the optimization of

the composition of currently used alloys. This method is also useful for measurements conducted on batteries using lead plated, reticulated current collectors.

ACKNOWLEDGEMENTS
This work was financially supported by Industrial Chemistry Research Institute through projects nr 841331, 841401.

References

1. D. Pavlov, Lead Acid Batteries. Science and Technology, 1st ed., Elsevier, (2011) Amsterdam, Netherlands.
2. A. J. Salkind, A. G. Cannone, F. A. Trumbure, Lead-Acid Batteries in**:** D. Linden, T. B. Reddy (Eds.), Handbook of batteries, 3rd ed., McGraw-Hill, (2001) New York, United States.
3. N. E. Bagshaw, *J. Power Sources* 53 (1995) 25.
4. R. Miraglio, L. Albert, A. El Ghachcham, J .Steinmetz, J. P. Hilger, *J. Power Sources* 53 (1995) 53.
5. D. Slavkov, B. Haran, B. Popov, F. Fleming, *J. Power Sources* 112 (2002) 199.
6. Z.W. Chen, J.B. See, W.F. Gillian, *J. Power Sources* 50 (1994) 47.
7. E. Rocca, , G. Bourguignon, J. Steinmetz, *J. Power Sources* 161 (2006) 666.
8. H.S. Panesar, in: D.H. Collins (Ed.), Power Sources, Vol. 3, Oriel Press, (1971) Newcastle-upon-Tyne, United Kingdom.
9. J.G. Sunderland, *J. Electroanal. Chem. Interfacial Electrochem*. 71 (1976) 341.
10. S. Fletcher, D.B. Matthews, *J. Electroanal. Chem. Interfacial Electrochem*. 126 (1981) 131.
11. R.L. Deutscher, S. Fletcher, J.A. Hamilton, *Electrochim. Acta* 31 (1986) 585.
12. A. Czerwinski, M. Zelazowska, M. Grden, K. Kuc, J.D. Milewski, A. Nowacki, G. Wojcik, M. Kopczyk, *J. Power Sources* 85 (2000) 49.
13. K. Darowicki, K. Andrearczyk, *J. Power Sources* 189 (2009), 988.
14. B. Zhang, J. Zhong, B. Zhang, Z. Cheng, *J. Power Sources* 196 (2011), 5719.
15. J. Lach, S. Obrębowski, A. Czerwiński, *J. Electroanal. Chem*. 742 (2015) 104.
16. M.M. Burashnikova, I.A. Kazarinov, I.V. Zotova, *J. Power Sources* 207 (2012) 19.
17. A. Nuzhny, *J. Power Sources* 158 (2006) 920.
18. S. Yandg, W. Zhao, S. Zhang, Patent CN104215545 A (2014).
19. J. Lach, A. Czerwiński, Patent RP pending P.416940 (2016).
20. A. Czerwiński, Z. Rogulski, S. Obrębowski, J. Lach, K. Wróbel, J. Wróbel, *Int. J. Electrochem. Sci.* 9 (2014) 4826.
21. S. S. Misra, *ECS Trans.* 41 (2014) 117.
22. E. Rocca, J. Steinmetz, *Electrochim. Acta* 44 (1999) 4611.
23. J. Xua, X. Liu, X. Li, E. Barbero, C. Dong, *J. Power Sources* 155 (2006) 420.
24. R. F. Nelson, D. M. Wisdom, *J. Power Sources*, 33 (1991) 165.
25. N. Bui, P. Mattesco, P. Simon, N. Pebere, *J. Power Sources* 73 (1998) 30.
26. C.S. Lakshmi, J.E. Manders, D.M. Rice, *J. Power Sources* 73 (1998) 23.
27. N. Bui, P. Mattesco, P. Simon, J. Steinmetz, E. Rocca, *J. Power Sources* 67 (1997) 61.
28. H. Giess, *J. Power Sources* 53 (1995) 31.
29. P. Ruetschi, B. D. Cahan, *J. Electrochem. Soc.* 104 (1957) 406.
30. B. K. Mahato, *J. Electrochem. Soc.* 126 (1979) 365.
31. M. Metikos-Hukovic, R. Babic, S. Brinic, *J. Power Sources* 64 (1997) 13.
32. S. Webster, P. J. Mitchell, N. A. Hampson, J. I. Dyson, *J. Electrochem. Soc.* 133 (1986) 134.
33. R. D. Prengaman, *J. Power Sources* 53 (1995) 207.

34. A. Czerwiński, M. Żelazowska, *J. Electroanal. Chem*. 410 (1996) 55.
35. A. Czerwiński, S. Obrębowski, J. Kotowski, Z. Rogulski, J.M. Skowroński, P. Krawczyk, T. Rozmanowski, M. Bajsert, M. Przystałowski, M. Buczkowska-Biniecka, E. Jankowska, M. Baraniak, J. Rotnicki, M. Kopczyk, *J. Power Sources* 195 (2010) 7524.
36. A. Czerwiński , S. Obrębowski, J. Kotowski, Z. Rogulski, J. Skowroński, M. Bajstert, M. Przystałowski, M. Buczkowska-Biniecka, E. Jankowska, M. Baraniak, J. Rotnicki, M. Kopczyk, *J. Power Sources* 195 (2010) 7530.
37. A. Czerwiński, Szymon Obrębowski, Zbigniew Rogulski, *J. Power Sources* 198 (2012) 378.
38. E. Gyenge, J. Jung, S. Splinter, A. Snaper, *J. Appl. Electrochem*. 32 (2002) 287.
39. E.Gyenge, J. Jung, B. Mahato, *J. Power Sources* 113 (2003) 388.
40. Y. Chen, B.-Z. Chen, X.-C. Shi, H. Xu, W. Shang, Y. Yuan, L.-P. Xiao, *Electrochim. Acta* 53 (2008) 2245.
41. Y. Chen, B.-Z. Chen, L.-W. Ma, Y. Yuan, *Electrochem. Commun*. 10 (2008) 1064.
42. Y. Chen, B.-Z. Chen, L.-W. Ma, Y. Yuan, *J. Appl. Electrochem*. 38 (2008) 1409.
43. L.-W. Ma, B.-Z. Chen, Y. Chen, Y. Yuan, *J. Appl Electrochem* 39 (2009).
44. A. Kirchev, N. Kircheva, M. Perrin, *J. Powers Sources* 196 (2011) 8773.
45. A. Kirchev, S. Dumenil, M. Alias, R. Christin, A. de Mascarel, M. Perrin, *J. Power Sources* 279 (2015) 809.
46. A. Kirchev, L. Serra, S. Dumenil, G. Brichard, M. Alias, B. Jammet, L. Vinit, *J. Power Sources* 299 (2015) 324.
47. Y.-I. Jang, N.J. Dudney, T.N. Tiegs, J.W. Klett, *J. Power Sources* 161 (2006) 1392.